Supplementary Methods

Cells culture and Reagents

MIO-M1 cells were a gift from Dr. Astrid Limb (University College London, Institute of Ophthalmology, London, United Kingdom). Isolation of primary Müller cells from mice was performed as previously described (1). To isolate human induced pluripotent stem cell (hiPSC)-derived Müller cells from retinal organoids (described below), two to four 120-day organoids were placed in a 15-ml conical tube, washed three times in high glucose DMEM containing 4.5 g/l of glucose (Invitrogen), and chemically digested with 0.5% trypsin (Life Technologies, Gibco-BRL) for 45 minutes at 37°C. The organoids were then washed again in high glucose DMEM and centrifuged for 5 minutes at 1000 RPM. The supernatant was discarded, and the organoids were mechanically disrupted with a 1 ml pipette. The cells were then plated and cultured as described below.

All cells were cultured in high glucose DMEM with 10% (vol/vol) FBS (Quality Biological) and 1% penicillin/streptomycin (Cellgro). Hypoxia chambers were used to expose cells and adult mouse retinal explants to 1% O_2. Digoxin was purchased from TOCRIS (Digoxin #4583/50). Desferrioxamine was obtained from Millipore Sigma (DFO#138-14-7). PT2385 was purchased from MedChemExpress.

Mice

Eight-week-old pathogen-free female C57BL/6 mice were obtained from Jackson Laboratory. Timed pregnant C57BL/6 mice were obtained from Charles River Laboratories. *rho*-

Gfp mice (2) were obtained from Dr. Don Zack (Johns Hopkins School of Medicine, Baltimore, MD).

Oxygen-induced Retinopathy (OIR) Model

OIR experiments were performed as previously described (3). Briefly, C57BL/6 mice were placed in 75% O_2 on P7. On P12, the mice were returned to room air and administered either digoxin by IP injection (2 mg/kg) or siRNA-containing nanoparticles by intravitreal injection. Mice with body weight less than 6 g at P17 were excluded from analysis. The data were collected from both males and females and the results combined, as there was no apparent difference between sexes. Representative images for selected time points from a minimum of three independent experiments are shown. Data from 3-8 pups were obtained at each time point.

Western Blot and ELISA

Cell and neurosensory retina lysates were subjected to 4–15% gradient SDS/PAGE (Invitrogen). Immunoblot assays were performed as previously described (4). Levels of secreted VEGF were measured in conditioned media from MIO-M1 cells using human VEGF ELISA kits (R&D System) according to the manufacturer's recommendations. Western blot scans and ELISAs are representative of at least three independent experiments.

Co-immunoprecipitation Assay

MIO-M1 cells were seeded in 10 cm dishes and cultured with DMEM supplemented with 10% FBS. Cells were placed in ambient (21% O_2) or hypoxic (1% O_2) conditions overnight and DMSO or PT2385 were added 8 hrs prior to cell lysing. Following hypoxic exposure, cells were

washed with cold PBS and quickly lysed in IP lysis buffer containing; 10 mM Tris-HCl, 150 mM NaCl, 1 mM EDTA, 0.5% NP-40, pH 8.0, and a freshly added 1x protease inhibitor, for 30 min. Samples were sonicated as previously described (5) and centrifugated at 13,000*g* for an additional 20 min at 4^{o}C to break nuclei. Immunoprecipitation was performed using primary antibodies against: ARNT/HIF-1b (H1beta234, Novus Biologics) added to 700 ug of supernatant and incubated with rotation at 4^{o}C for 16 hours. Protein A/G Sepharose beads were added and samples were rotated for 2 hours at 4^{o}C. Beads were precipitated, washed with lysis buffer and samples were denatured for western blotting analysis. Antibodies and IgG used: mouse ARNT/HIF-1b antibody (H1beta234) (Novus Biologicals), rabbit ARNT/HIF-1b antibody (Novus Biologicals), rabbit HIF-2a/EPAS1 antibody (Novus Biologicals), rabbit HIF-1a/ Antibody (Cayman Chemical), normal mouse IgG (Santa Cruz Biotechnology).

Reverse Transcription and Quantitative Real-Time PCR (RT-qPCR)

Primers are listed in Supplemental Table 2.

Total RNA was isolated from culture cells or retinas with PureLink^{TM} RNA Mini Kit (Invitrogen #12183025), and cDNA was prepared with MuLV Reverse Transcriptase (Applied Biosystems). Quantitative real-time PCR was performed with Power SYBR Green PCR Master Mix (Applied Biosystems) and MyiQ Real-Time PCR Detection System (Bio-Rad). Normalization was done using cyclophilin A for mouse tissue and cell lines and β-actin for human cell lines.

Adenoviral vectors

Adenovirus expressing LacZ control (Ad-LacZ) and expressing HIF-1α (Ad-CA5) have

been previously described (6). MIO-M1 cells were infected with Ad-Ca5 or Ad-LacZ ($2x10^{10}$ adenoviral particles per mL of culture media) for 24 hours, after which the media was removed and the cells washed three times with PBS prior to being used in experiments. Ten-week-old male C57BL/6 mice were subjected to intraocular injections of 1 µl of Ad-CA5, containing $2x10^{10}$ adenoviral particles, into the right eye and Ad-LacZ control into the left eye as described below. Mice were sacrificed 6 days after intraocular injections, retina flat mounts and OCT-embedded fixed frozen cross sections were made, and isolectin-B4 (Thermo Fisher), CD-31 (Abcam) and HIF-1α (Novus) staining were carried out (as described below). To assess vessel length, 10-12 high powered fields were randomly selected and total length of vessels (isolectin-B4) was measured and analyzed by AngioTool.

Immunofluorescence

Details for antibodies are provided in Supplemental Table 1.

Immunofluorescence assays in MIO-M1 cells and primary mouse retinal Müller cells were performed as previously described (4, 7, 8). Human retinal organoids were fixed in 4% paraformaldehyde for 1 hour, washed in PBS (2 × 5 min), and cryoprotected with a sucrose gradient (6.75%, 12.5%, and 25%, overnight at 4°C each) with a final incubation in 25% sucrose/OCT (2:1 ratio respectively) for 1 hour at room temperature (RT). Samples were embedded in 25% sucrose/OCT Tissue-Tek (Sakura), frozen, and stored at -80°C until used. Cryosections of 12-16 µm thickness were obtained and collected on Superfrost Plus slides. Sections were air dried for 1 hour, washed in PBS (3 × 5 min), blocked in 10% goat serum in PBS with 0.25% Triton X-100 for 1 hour at RT, and incubated overnight with a primary antibody in 2% goat serum in PBS with 0.05% Triton X-100 at 4°C. The next day, the slides were washed in

PBS (3 × 5 min) and incubated with an Alexa Fluor-conjugated secondary antibody (1:500; Molecular Probes) in PBS for 1 hour in the dark at RT. The slides were then washed in PBS (3 × 5 min), incubated in DAPI (1:1000 in PBS) for 10 min, and cover-slipped using DAKO fluorescent mounting medium. Similar procedures were applied for double and triple immunostaining. Fluorescence images were acquired with a Nikon C2 laser scanning confocal microscope (Melville, NY). The images were minimally processed using Adobe Photoshop CS5 (San Diego, CA)

The immunohistochemistry assay of cryopreserved mouse retina tissue sections was performed as previously described (4, 7, 8). Briefly, isolated retinas from mice were fixed in 4% paraformaldehyde for 2 hours. After washing in buffered saline, the tissues were embedded in OCT containing 6% agarose (w/v) and 10-μm-thick slices were cut. To ensure that cross sections included both posterior (ischemic) retina as well as anterior (perfused) retina, sections tangential, but just anterior, to the optic nerve were obtained, and CD31-labeling of retinal vasculature was used as an anatomical landmark for the presence or absence or vessels. For double-labeling, the slices were incubated in a blocking solution consisting of 5% normal donkey serum and 0.3% Triton X-100 in saline for 1 hour at RT. Subsequently, the slices were incubated in a mixture of primary antibodies overnight at 4° C. After washing, the slices were incubated in secondary antibodies for 1 hour at RT. Control slices were stained with IgG. Immunofluorescence was performed using donkey anti-mouse Alexa Fluor 488/555, donkey anti-goat Alexa Fluor 647 or donkey anti-rabbit Alexa Fluor 488/555, in combination with DAPI (Invitrogen). Images were captured by a Zeiss LSM 710 confocal microscope or an EVOS FL Auto 2 Imaging System (Thermo Fisher Scientific, Waltham, MA).

For quantitation of retinal neovascularization in retinal flat mounts of mice, animals were sacrificed at the designated time points using CO_2 asphyxiation, and eyes of mice were enucleated

and fixed with a solution of 4% paraformaldehyde in PBS (Thermo Scientific™) for two hours at RT, followed by washing with PBS for 10 minutes in a shaker. Retinas were then isolated and incubated in 0.5% BSA solution overnight at 4ºC. Retinas were washed with PBS 3 times for 10 minutes in the shaker and then stained with isolectin B4 (Invitrogen; 1:200 dilution in PBS) overnight in 4ºC. After washing 3 times for 10 minutes each in the shaker, the retinas were mounted. Images were captured at high magnification (40X) with Zeiss fluorescent microscope. The images were selected (8 fields per eye, 2 fields per petal, including area of neovascularization) and fluorescence intensity was measured by ImageJ software (NIH).

HypoxyProbe

Eyes from OIR mice were harvested 90 minutes after Hypoxyprobe™-1 (60 mg/kg body weight) was administered. Retina flat mounts and OCT-embedded fixed frozen whole eye cross sections were made, and anti-CD-31 antibody (R&D) staining were carried out. Retina flat mounts and whole eye cross sections were washed three times with for 5 minutes in PBS and then incubated for 90 min with Cy-3-conjugated goat anti-mouse antibody 1:150 (Jackson Immuno Research Laboratories). After three additional washes for 5 minutes in PBS, sections were incubated to 90 minutes with anti-Goat 1:500 (Invitrogen).

Hematoxylin and Eosin staining

Retinal organoids were fixed in Davidson's fixative solution O/N, treated with buffered formalin and embedded in paraffin by standard procedures. Briefly, retinal organoids were processed through graded alcohols (70-100%) and cleared in xylene before being embedded in paraffin. 5-micron sections were cut from the paraffin blocks by microtome and mounted onto

slides. The sections were deparaffinizing by xylene and rehydrated using graded alcohols (100%-70%) and stained using routine hematoxylin and eosin (H&E) staining, followed by dehydration through graded alcohols (70%-100%) and xylene. These sections were then mounted in cytoseal. Morphology was characterized by light microscopy using a Nikon Eclipse 80i microscope fitted to a Nikon DS-Fi1 camera.

In situ hybridization

RNA in situ hybridization was performed with RNAscope® 2.5 HD Duplex Detection Reagent Kit (ACD, #323350) following the manufacturer's protocol. Fresh eyecups, without prior fixation, were embedded in OCT compound (Tissue-Tek), immediately frozen in liquid nitrogen, sectioned at a thickness of 14 μm, and assayed using a probe specific for *Vegf* mRNA (#405131) or a negative control probe (#320751). The signal was visualized and captured by a meta 710 LSM confocal microscope (Carl Zeiss Inc., Thornwood NY).

Immunohistochemistry

Details for antibodies are provided in Supplemental Table 1.

Immunohistochemical detection of human paraffin-embedded tissue sections using premixed biotinylated anti-rabbit, anti-mouse and anti-goat immunoglobulins in phosphate buffered saline (PBS) from an ABC system (Dako, Santa Clara, CA) performed according to the manufacturer's protocols as previously described (9, 10). All immunohistochemical reagents, including antibodies, were identical for all specimens. Images were captured by scanning slides using the Aperio ScanScope program on Aperio ScanScope XT® System (Leica Biosystems, Wetzlar, Germany).

Nanoparticles

Reducible branched ester amine quadpolymers (rBEAQs) were synthesized as previously described (11). Briefly, bioreducible monomer 2,2-disulfanediylbis (ethane-2,1-diyl) diacrylate (BR6), diacrylate monomer bisphenol A glycerolate (1 glycerol/phenol) diacrylate (B7), tri-acrylate monomer trimethylolpropane triacrylate (B8), and side chain monomer 4-amino-1-butanol (S4) were reacted overnight at 90ºC with stirring to form the acrylate-terminated base polymer, which was then end-capped with 2- (3-aminopropylamino)ethanol (E6) to form the final polymer used in these studies. siRNA-encapsulated nanoparticles were formed by dissolving siRNA and polymer at the desired concentrations in 25 mM sodium acetate solution (NaAc; pH 5) and mixing the two solutions at a 1:1 volume ratio. Nanoparticles were allowed to self-assemble for 10 minutes at RT, at which time they were mixed at a 1:1 volume ratio with sodium bicarbonate solution at a final concentration of 9 mg/mL (107 mM $NaHCO_3$; pH 9).

To determine nanoparticle size and surface charge in neutral isotonic buffer, particle solutions were diluted in 150 mM PBS. Hydrodynamic diameter was measured via dynamic light scattering (DLS) at 1:6 dilution in PBS using a Zetasizer NanoZS (Malvern Panalytical) and via nanoparticle tracking analysis (NTA) at 1:500 dilution in PBS using a NanoSight NS300. Zeta potential was measured also at 1:6 dilution in PBS via electrophoretic light scattering on the same Zetasizer instrument. Transmission electron microscopy (TEM) images were acquired with a Philips CM120 (Philips Research). Nanoparticles were prepared at a polymer concentration of 1.8 mg/mL in sodium acetate buffer, and 30 μL nanoparticle solution were added to 400-square mesh carbon coated TEM grids and allowed to coat grids for 20 minutes. Grids were then rinsed with

ultrapure water, counterstained with uranyl acetate (0.5% in distilled water) and allowed to fully dry before imaging.

Nanoparticle knockdown was screened in NIH-3T3 cells made to constitutively express destabilized GFP (GFPD2; 2 hour half-life) using a PiggyBac transposon/transposase system, as previously described (11). For transfection, cells were seeded on 96 well tissue culture plates at a density of 12,000 cells per well in 100 μL complete medium and allowed to adhere overnight. Nanoparticles were formed immediately prior to transfection, with each nanoparticle condition formulated with scrambled control RNA (scRNA) or an siRNA targeting GFP (siGFP) at a polymer-to-RNA weight ratio of 20 w/w. Nanoparticles were added to cells in complete serum media at the siRNA dosage indicated and incubated for 4 hours, at which point the nanoparticle/media mixture was replaced with fresh complete media.

GFPd2 knockdown was assessed via flow cytometry one day post transfection using a BD Accuri C6 flow cytometer (BD Biosciences). Knockdown was quantified by normalizing the fraction of GFP+ cells in wells treated with siGFP to that of wells treated with scRNA using the same nanoparticle formulation. Knockdown was also visualized using an AxioObserver.A1 fluorescence inverted microscope (Zeiss).

For *in vitro* transfections, nanoparticle solutions were added directly to cell culture media and incubated for 4 hours. Nanoparticles were formulated at a polymer: siRNA wt/wt ratio of 20; the final siRNA dose was 100 nM per well. For transfections simultaneously knocking down HIF-1α and HIF-2α, siRNA targeting each sequence was pre-mixed at a 1:1 molar ratio prior to mixing with polymers; siRNA dose in this case was 50 nM per well per siRNA sequence.

For *in vivo* intravitreal injections, nanoparticles were synthesized at a polymer concentration of 5 mg/mL to enable a higher dose to be delivered in the limited injection volume. Nanoparticles were lyophilized in the presence of sucrose (30 mg/mL) as a cryoprotectant and resuspended using deionized water to a final isotonic sucrose concentration of 100 mg/mL immediately prior to injection.

Intraocular Injections

Intravitreal injections were performed with a PLI-100A Pico-liter Microinjector (Warner Instruments, Harvard Bioscience) using pulled-glass micropipettes. Each micropipette was calibrated to deliver a 1 µl volume on depression of a foot switch. The mice were anesthetized with a ketamine (100 mg/kg) and xylazine (5mg/kg) mixture, and under a dissecting microscope, the sharpened tip of the micropipette was passed through the sclera just posterior to the limbus into the vitreous cavity and the foot switch was depressed, which caused fluid to penetrate into the vitreous space.

Intraperitoneal Injections

Intraperitoneal (IP) injection of digoxin (2 mg/kg) was performed using an insulin syringe. Digoxin was injected into the peritoneal cavity of neonatal C57BL/6 mice at postnatal day 12 (P12) or P13, and the retinal vasculature was assessed at P17.

Oral gavage

Oral gavage with PT2385 (30 mg/kg) was performed twice daily for 5 consecutive days in the OIR model. PT2385 was dissolved in DMSO (20 mM), diluted in 0.5% methylcellulose, 0.5%

Tween 80, 0.1% NaCl in water (w/v), and administered daily to C57BL/6 mice from P12 to P16. The dosing volume was 10 mL/kg.

Supplementary References

1. Wahlin KJ, Lim L, Grice EA, Campochiaro PA, Zack DJ, and Adler R. A method for analysis of gene expression in isolated mouse photoreceptor and Muller cells. *Molecular vision.* 2004;10:366-75.
2. Chan F, Bradley A, Wensel TG, and Wilson JH. Knock-in human rhodopsin-GFP fusions as mouse models for human disease and targets for gene therapy. *Proc Natl Acad Sci U S A.* 2004;101(24):9109-14.
3. Smith LE, Wesolowski E, McLellan A, Kostyk SK, D'Amato R, Sullivan R, et al. Oxygen-induced retinopathy in the mouse. *Invest Ophthalmol Vis Sci.* 1994;35(1):101-11.
4. Xin X, Rodrigues M, Umapathi M, Kashiwabuchi F, Ma T, Babapoor-Farrokhran S, et al. Hypoxic retinal Muller cells promote vascular permeability by HIF-1-dependent up-regulation of angiopoietin-like 4. *Proceedings of the National Academy of Sciences of the United States of America.* 2013;110(36):E3425-34.
5. Gong F, Chiu LY, Cox B, Aymard F, Clouaire T, Leung JW, et al. Screen identifies bromodomain protein ZMYND8 in chromatin recognition of transcription-associated DNA damage that promotes homologous recombination. *Genes Dev.* 2015;29(2):197-211.
6. Kelly BD, Hackett SF, Hirota K, Oshima Y, Cai Z, Berg-Dixon S, et al. Cell type-specific regulation of angiogenic growth factor gene expression and induction of angiogenesis in nonischemic tissue by a constitutively active form of hypoxia-inducible factor 1. *Circ Res.* 2003;93(11):1074-81.
7. Babapoor-Farrokhran S, Jee K, Puchner B, Hassan SJ, Xin X, Rodrigues M, et al. Angiopoietin-like 4 is a potent angiogenic factor and a novel therapeutic target for patients

with proliferative diabetic retinopathy. *Proceedings of the National Academy of Sciences of the United States of America.* 2015;112(23):E3030-9.

8. Rodrigues M, Xin X, Jee K, Babapoor-Farrokhran S, Kashiwabuchi F, Ma T, et al. VEGF secreted by hypoxic Muller cells induces MMP-2 expression and activity in endothelial cells to promote retinal neovascularization in proliferative diabetic retinopathy. *Diabetes.* 2013;62(11):3863-73.
9. Montaner S, Sodhi A, Molinolo A, Bugge TH, Sawai ET, He Y, et al. Endothelial infection with KSHV genes in vivo reveals that vGPCR initiates Kaposi's sarcomagenesis and can promote the tumorigenic potential of viral latent genes. *Cancer cell.* 2003;3(1):23-36.
10. Rodrigues M, Kashiwabuchi F, Deshpande M, Jee K, Goldberg MF, Lutty G, et al. Expression Pattern of HIF-1alpha and VEGF Supports Circumferential Application of Scatter Laser for Proliferative Sickle Retinopathy. *Invest Ophthalmol Vis Sci.* 2016;57(15):6739-46.
11. Rui Y, Wilson DR, Sanders K, and Green JJ. Reducible Branched Ester-Amine Quadpolymers (rBEAQs) Codelivering Plasmid DNA and RNA Oligonucleotides Enable CRISPR/Cas9 Genome Editing. *ACS Appl Mater Interfaces.* 2019;11(11):10472-80.

Supplementary Figure Legends

Supplemental Figure 1. Calculation of retinal ischemic index in sickle cell patients using ultrawidefield fluorescein angiography (UWF FA).

(**A**) UWF FA images (example from Figure 2A) were obtained from patients with documented sickle cell disease (SS, SC, or Sßthal). (**B**) Two investigators independently outlined the margin between perfused and nonperfused retina (red line) and the extent of visible nonperfused retina (blue line). (**C**) Areas of perfused retina at the margin of the image (purple line) or areas obstructed by ocular adnexa (lid margin, lashes, etc.) were also outlined (white line) to calculate the area of perfused retina (red hashed area) and the area of nonperfused retina (blue hashed area). The retinal ischemic index was calculated by dividing the area of the ischemic retina by the total area of retina (ischemic + perfused) visible in the image.

Supplemental Figure 2. Comparison of retinal ischemic index of 55 sickle cell eyes measured by two independent graders.

Retinal ischemic index was calculated independently by two independent graders (YQ and MM) for all 55 eyes of the 28 patients. Pearson correlation coefficient was computed between the corresponding indices generated by the two separate graders The interclass correlation between the two graders was 0.96.

Supplemental Figure 3. Engineering and characterization of nanoparticle-mediated RNAi.

(A) Monomer structures. (**B)** Reaction scheme for reducible branched ester amine quadpolymers (rBEAQ). (1) Acrylate-terminated rBEAQ is synthesized via Michael addition of B and S monomers; (2) Polymer end-capping with monomer E6 yields final polymer products. (**C)** rBEAQ

polymer nanoparticle hydrodynamic diameter as measured by nanoparticle tracking analysis and zeta potential as measured by electrophoretic mobility. Data represented as mean + SEM, n=3. **(D)** Representative rBEAQ polymer nanoparticle size distribution from nanoparticle tracking analysis (NTA) shown in the histogram. **(E)** Transmission electron microscopy image of rBEAQ-siRNA nanoparticles.

Supplemental Table 1. Antibodies used in this study.

Name	Company	Species	Catalog Number	dilution	Marker/Applications
HypoxyProbe	HPI	rabbit	PAb2627AP	1:20	IF (hypoxia)
HIF-1α	Gene Tex	rabbit	GTX127309	1:200-1:1000	WB/IF
HIF-1α	Cayman	rabbit	10006421	1:1000	CoIP
H1beta234	Novus	mouse	NB100-124	1:1000	CoIP
HIF-1β	Novus	rabbit	NB100-110	1:1000	WB
HIF-2α	Gene Tex	mouse	GTX632015	1:200-1:1000	WB/IF
β-Actin	Cell signaling	rabbit	4967	1:5000	WB
GAPDH	MilliporeSigma	mouse	G8795	1:10000	WB
RPE65	abcam	mouse	ab13826	1:5000	WB
Vimentin	abcam	goat	ab11256	1:50	WB/IF
Vimentin	abcam	rabbit	ab45939	1:1000	IF
CRALBP	abcam	mouse	ab15051	1:500	IF
GFAP	abcam	goat	ab53554	1:500	IF
Isolectin GS IB4	Thermo Fisher		I21413	1:200	IF
HIF-1α	Thermo Fisher	rabbit	PA1-16601	1:1000	IF
HIF-1α	Novus	mouse	NB-100-105	1:500	IF
HIF-2α	Novus	rabbit	NB-100-122	1:200-1000	IF/ CoIP
HIF-2α	Novus	mouse	NB-100-132	1:100/1:1000	IF/IHC
HIF-2α	R&D	goat	AF2997	1:200	IF
GS	abcam	mouse	ab64613	1:500	IF
GS	MilliporeSigma	mouse	MAB302	1:200	IF
CD31	R&D	goat	AF3628	1:1000	IF
CD31	abcam	Rat	ab25563	1:50	IF
REC	MilliporeSigma	rabbit	AB5585	1:500	IF
PAX-6	DSHB	mouse	AB_528427	1:50	IF
CD34	Novus	mouse	NB-500-608	1:500	IHC
HIF-1α	abcam	rabbit	ab2185	1:500	IHC
VEGF	Santa Cruz	rabbit	sc-152	1:1000	IHC
ANGPTL4	abcam	rabbit	ab115798	1:400	IHC
normal mouse IgG	Santa Cruz		sc-2025		CoIP
secondary antibodies	Invitrogen			1:1000	IF
secondary antibodies	Dako			1:100	IHC

Supplemental Table 2. Primer sequences for Real-Time (RT)-PCR

	Gene		Sequence (5'to 3')
Mouse			
	ANGPTL4	Forward	TTGGTACCTGTAGCCATTCC
		Reverse	GAGGCTAAGAGGCTGCTGTA
	VEGF	Forward	CTTATACAGGAATGGAGGCTGT
		Reverse	TTCACCTGACAGGATTGGATAAT
	Cyclophilin A	Forward	AGCATACAGGTCCTGGCATC
		Reverse	TTCACCTTCCCAAAGACCAC
	HIF-1α	Forward	GCACGGGCCATATTCATGTC
		Reverse	CACGTCATGGGTGGTTTCTTG
	HIF-2α	Forward	CTGAGGAAGGAGAAATCCCGT
		Reverse	TGTGTCCGAAGGAAGCTGATG
	GFP	Forward	AGCATACAGGTCCTGGCATC
		Reverse	TTCACCTTCCCAAAGACCAC
Human			
	ANGPTL4	Forward	GGACACGGCCTATAGCCTG
		Reverse	CTCTTGGCGCAGTTCTTGTC
	VEGF	Forward	GGGCAGAATCATCACGAAGT
		Reverse	TGGTGATGTTGGACTCCTCA
	β-actin	Forward	CTCTTCCAGCCTTCCTTCCT
		Reverse	AGCACTGTGTTGGCGTACAG

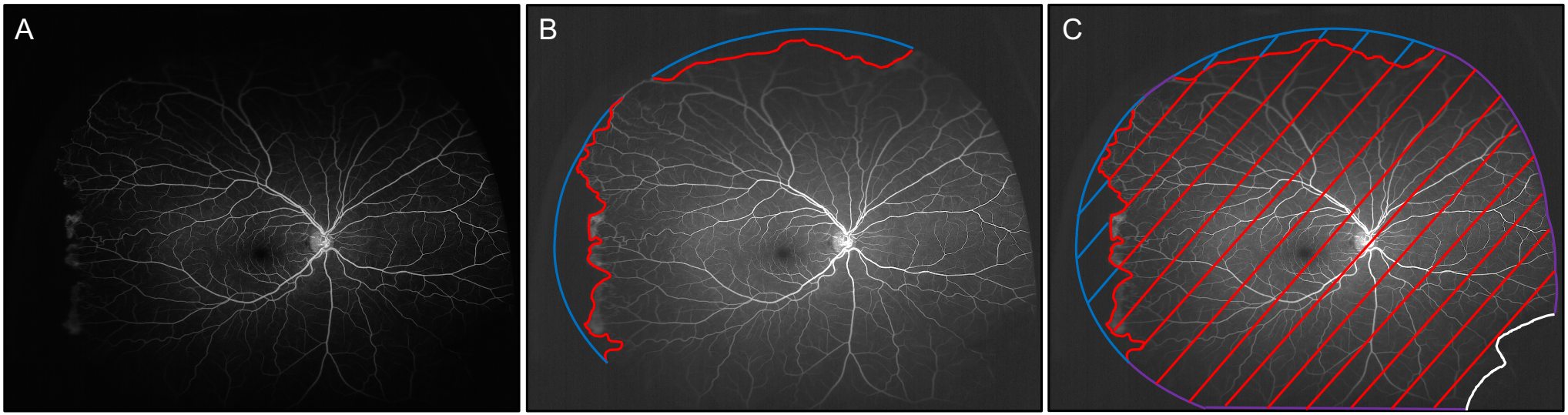
A
B
C

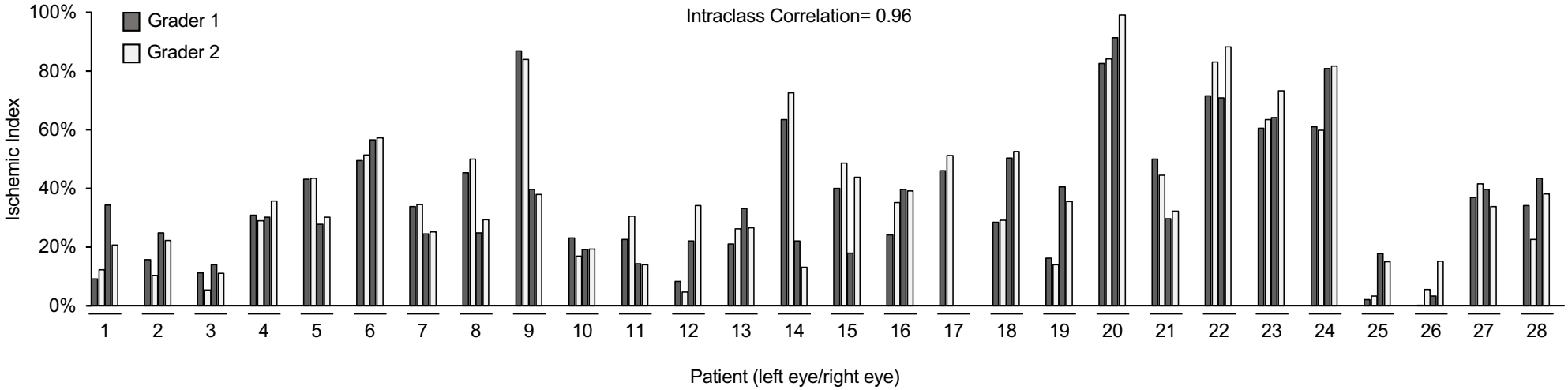
Grader 1
Grader 2
Intraclass Correlation= 0.96
Ischemic Index
100%
80%
60%
40%
20%
0%
1
2
3
4
5
6
7
8
9
10
11
12
13
14
15
16
17
18
19
20
21
22
23
24
25
26
27
28
Patient (left eye/right eye)

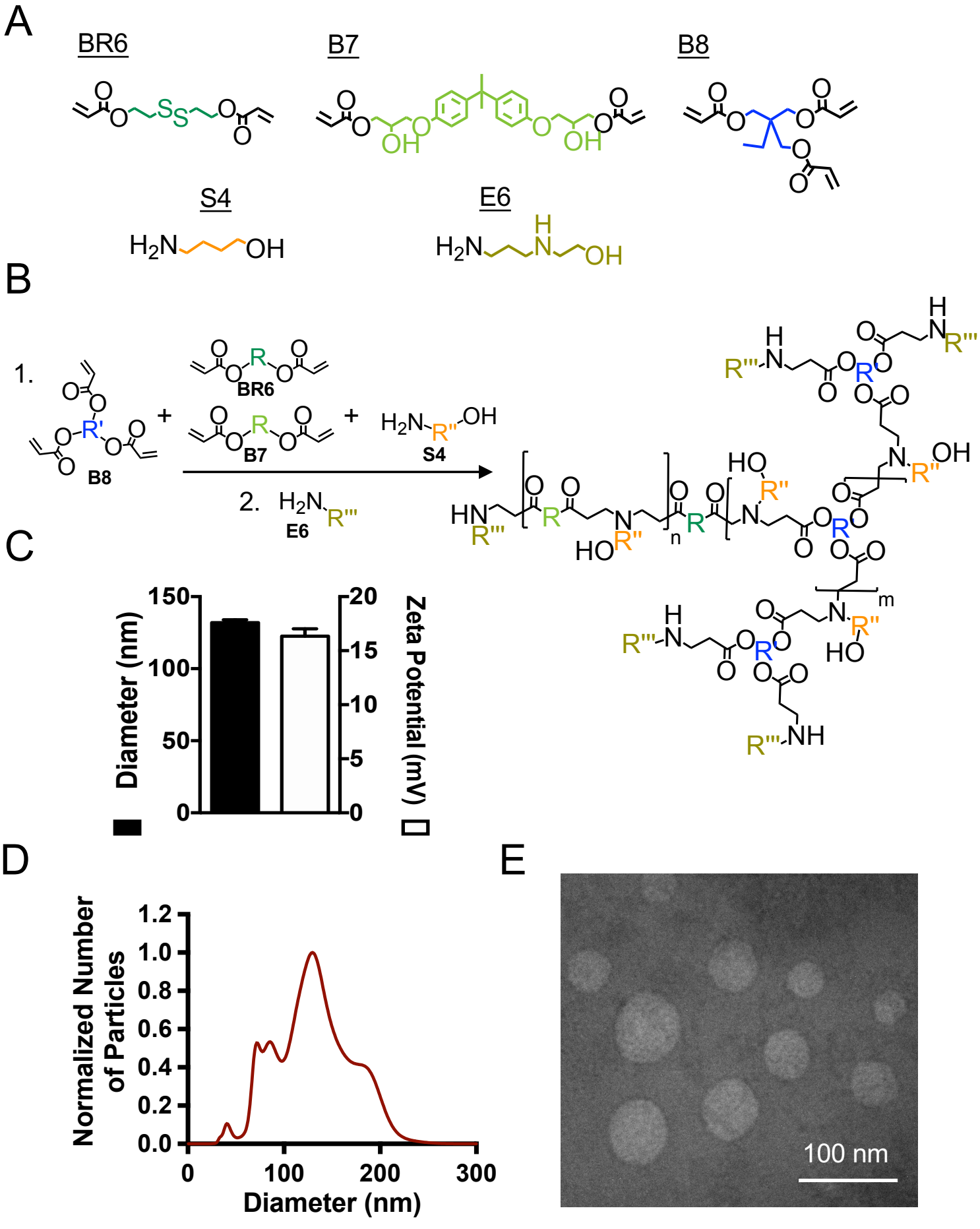
A
BR6
B7
B8
S4
E6
B
1.
BR6
B7
B8
S4
2.
E6
C
Diameter (nm)
Zeta Potential (mV)
150
100
50
0
20
15
10
5
0
D
Normalized Number of Particles
1.2
1.0
0.8
0.6
0.4
0.2
0.0
0
100
200
300
Diameter (nm)
E
100 nm